iScience, Volume *26*

Supplemental information

In-cell investigation of the conformational landscape of the GTPase UreG by SDSL-EPR

Annalisa Pierro, Ketty Concetta Tamburrini, Hugo Leguenno, Guillaume Gerbaud, Emilien Etienne, Bruno Guigliarelli, Valérie Belle, Barbara Zambelli, and Elisabetta Mileo

Supplementary Information

Figure S1: Confirmation of the labeling reaction by MALDI-Tof Mass spectrometry, related to Figure 1.

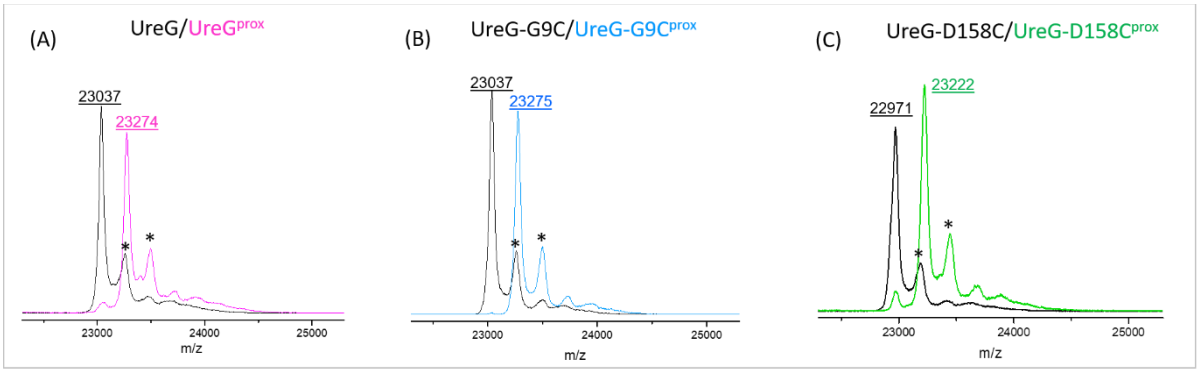

Mass spectrometry (MALDI-ToF) was performed to confirm the protein labeling with M-proxyl.
The mass increments observed for UreG wt (A) and G9C variant (B) perfectly match the value expected for the grafting of one molecule of M-proxyl per protein (+237 Da). In the case of the variant D158C (C) the mass increment is slightly higher (+251 Da) than expected, however the shape of the mass spectrum is very similar to those obtained for the other variants and considering the error of the measurement, we can confirm the correct labeling.
The small peaks (indicated by black stars in the figure) of ~210 Da correspond to the formation of adducts with the sinapinic matrix (206 Da).
Sample preparation: Samples of ~80 pmol of unlabeled SpUreG and labeled SpUreG were prepared by dilution in 10 µL of 0,1 % of trifluoro-acetic acid (TFA) in water (v/v) before being spotted onto a MALDI target plate (1 µL). A saturated solution of sinapic acid matrix (1 µL) in 70 % acetonitrile/water, 0,1% TFA (v/v) was added. The global mass was measured on a MALDI-ToF mass spectrometer Microflex II from Bruker Daltonics in the range of 2000 to 65000 Da in a positive linear mode. External mass calibration was performed using the signals from the Protein standard I (Bruker Daltonics). The error on the measurement is of +/- 5 Da.

Figure S2: Protein delivery by heat-shock, related to Figure 2 and 3.

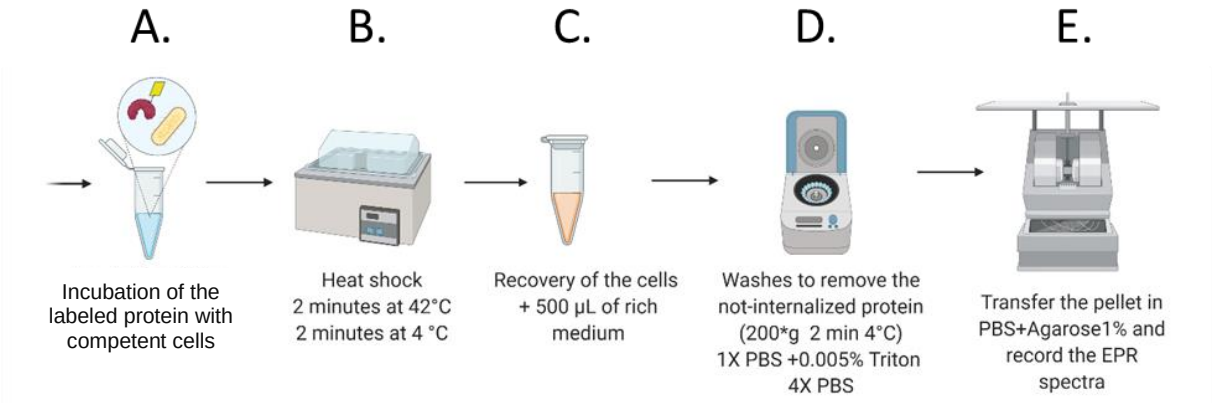

(A) a mixture of 20 µL of competent cells and 20 µL of labeled protein (~800 µM) are incubated on ice for 10 minutes.

As a drastic loss of cell competence is observed once the cells are stored at -80 °C, the experiments need to be performed on freshly prepared cells.

(B) the mixture is incubated 2 minutes at 42 °C and 2 minutes at 4 °C.

(C) After the shock, the cells are recovered by addition of 500 µL of pre-warmed reach medium (SOC).

(D) Cells are then washed by centrifugation at 3200 $x\ g$, 2 minutes at 4 °C until the not internalized protein is completely removed.

(E) The cell pellet is resuspended in 50 µL of PBS + 1% LT-Agarose and transferred in an EPR quartz capillary.

Figure S2 created with BioRender.com.

Figure S3: Heat-shock experiment in absence and in presence of Ca(II) ions, related to Figure 2 and 3.

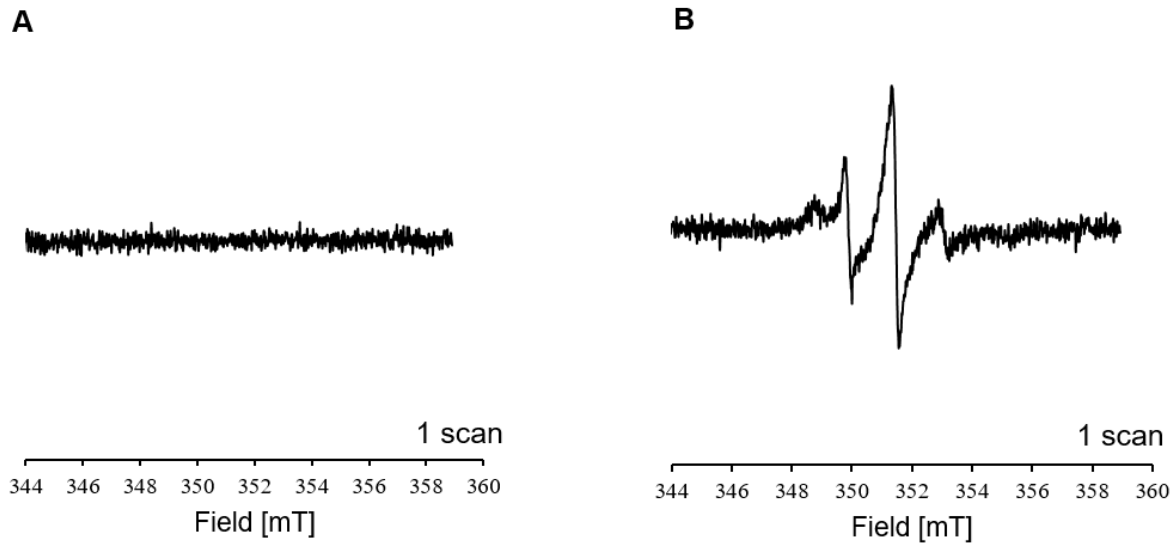

Room temperature CW EPR spectrum of an *E. coli* cell sample containing cells and *Sp*UreG^{proxyl} which was subjected to a thermal shock in the absence (**A**) or presence of 10 mM $CaCl_2$ (**B**).

Figure S4: Protein delivery by heat-shock, related to Figure 3.

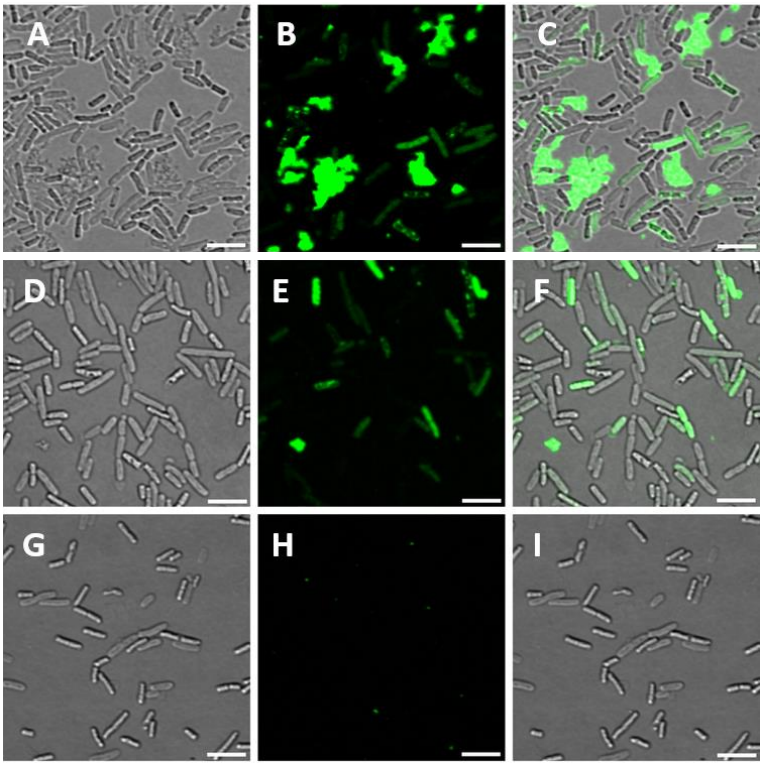

(A, D, G) Transmission (DIC) and (B, E, H) Fluorescence (MIP) images of sfGFP delivered in bacteria by heat-shock in the presence of $CaCl_2$ 50 mM (A, B, C) and $CaCl_2$ 10 mM (D, E, F). Panels G, H, I are related to the control experiment in which the suspension containing bacteria and sfGFP are not subjected to the heat-shock. Scale bars represent 2 µm.

Figure S5: Ratio of average fluorescence, measured in each bacterium, to the background image, related to Figure 3.

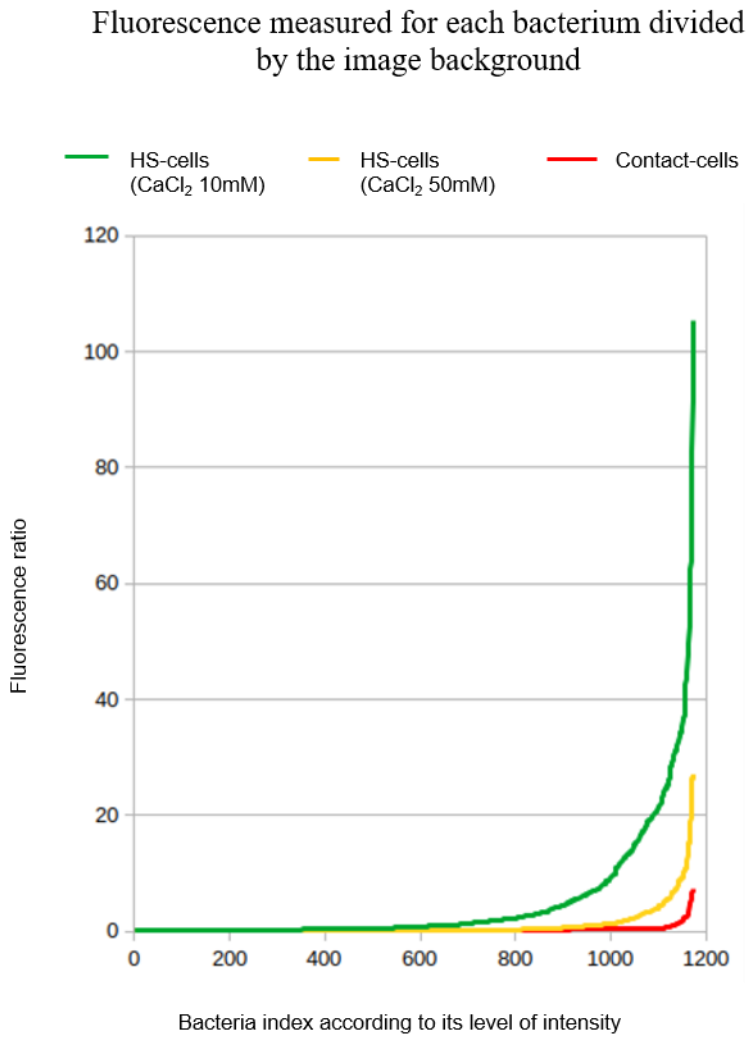

The average fluorescence, measured in 1200 bacteria, normalized to the background of the image, sorted in ascending order for bacteria treated with 10mM (green) and 50 mM (yellow) $CaCl_2$ that underwent heat-shock and bacteria that remained just in contact (red) with *Sf*GFP.

Figure S6: Control experiments without heat-shock application, related to Figure 2 and 3.

Non-specific interaction of the protein with the cell membrane was investigated analyzing by EPR spectroscopy a sample containing cells and *Sp*UreG (C68^{proxyl}) which was not subjected to a thermal shock in the presence of 10 mM $CaCl_2$. This sample is then recovered, washed and suspended in 50 µL of PBS buffer as described previously. The supernatants and the cells are analyzed by EPR at room temperature. No EPR signal was detected associated with cells.

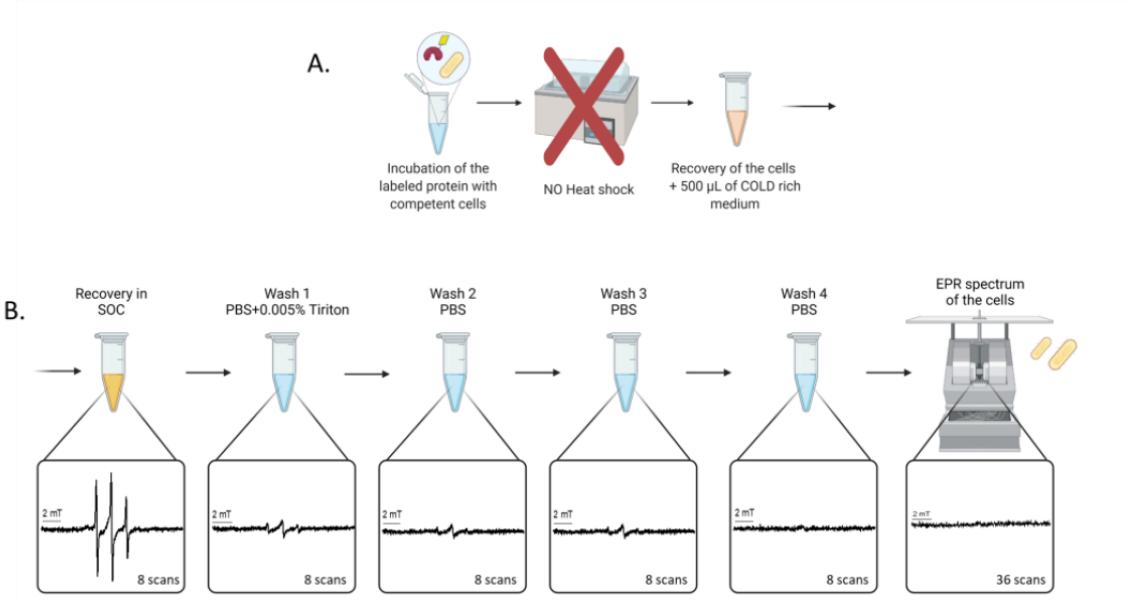

A. Protein sample is UreG-C68^{proxyl} is incubated with competent *E. coli* cells and no heat shock is applied. All the material is kept at 4 °C. **B.** EPR spectra of the supernatants collected after recovery, at each washing step. The last panel shows the EPR spectrum of *E. coli* cells after the washes. Created with BioRender.com.

Figure S7: Cell viability, related to Figure 3.

We tested the viability of cells exposed to heat shock or kept on ice 'in contact' with 350 µM of *sf*GFP. The cells were both washed and resuspended in 50 µL of PBS, following the reported protocol for EPR sample preparation. Duplicates were prepared for each of these two conditions, and all the samples were left in PBS for 10 minutes to simulate the recording time of an EPR experiment.

To begin the experiment, we filled a 96-well plate with 190 µL of LB under sterile conditions. Next, we transferred 10 µL from the cell solutions into the first well. Subsequently, we performed serial dilutions by transferring 10 µL from the previous well into the adjacent well on the right. This procedure resulted in a line of wells containing 12 dilutions of the in-cell or in contact samples in LB. As a sterility control, one line of the plate was filled with LB alone.

For the growth test on solid medium, we spotted 2 µL of each diluted sample onto a petri dish pre-filled with LB Agar and incubated it overnight at 37 °C (Figure A). To monitor the growth of cells in liquid medium, we placed the same 96-well plate in a Tecan reader and recorded the OD_{600} over a 14-hour period at 37 °C (Figure B). In both cases, the sample exposed to thermal treatment exhibited similar viability to the sample in contact with the protein.

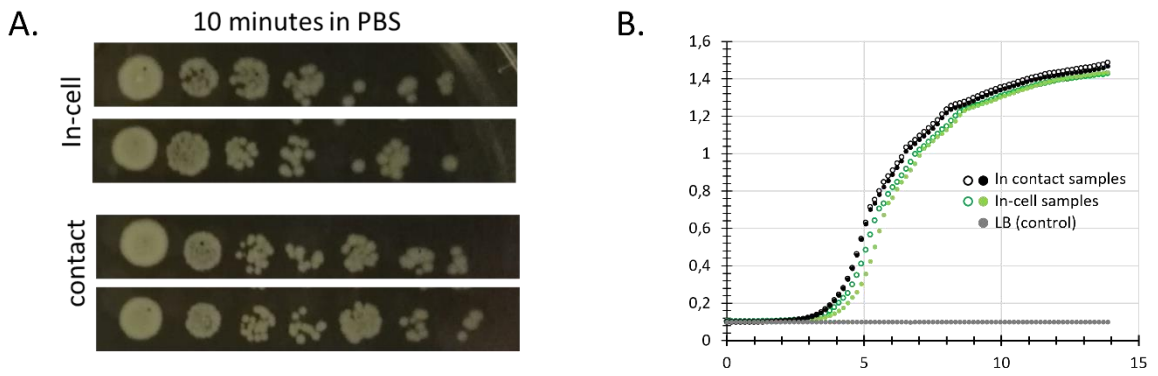

Table S1: Table resuming EPR spectra simulation results, related to Figure 2.

		In vitro		In-cell		Δ τ_c ($\tau_{c\ in\ cell}$ - $\tau_{c\ in\ vitro}$) (ns)		Δ *weight* (*weight* $_{in\ cell}$ - *weight* $_{in\ vitro}$)
Variant		Component *sharp*	Component *broad*	Component *sharp*	Component *broad*	Component *sharp*	Component *broad*	Component *broad*
G9C	τ_c (ns)	0.20 (± 0.02)	6.54 (± 0.65)	0.41 (± 0.04)	8.58 (± 0.86)	+ 0.21	+ 2.04	+ 10%
	weight	21% (± 1)	79% (± 4)	11% (± 1)	89% (± 5)			
C68	τ_c (ns)	0.45 (± 0.04)	4.00 (± 0.40)	0.49 (± 0.05)	6.40 (± 0.64)	+0.04	+ 2.40	+14%
	weight	50% (± 3)	50% (± 3)	36% (± 2)	64% (± 3)			
D158C	τ_c (ns)	0.36 (± 0.04)	5.53 (± 0.55)	0.52 (± 0.05)	7.25 (± 0.72)	+ 0.16	+ 1.72	+6%
	weight	25% (± 1)	75% (± 4)	19% (± 1)	81% (± 4)			

The error for τ_c and weight values is indicated in the brackets.

Figure S8: EPR spectra of UreG variants in the presence of different crowders and related simulation results, related to Figure 2.

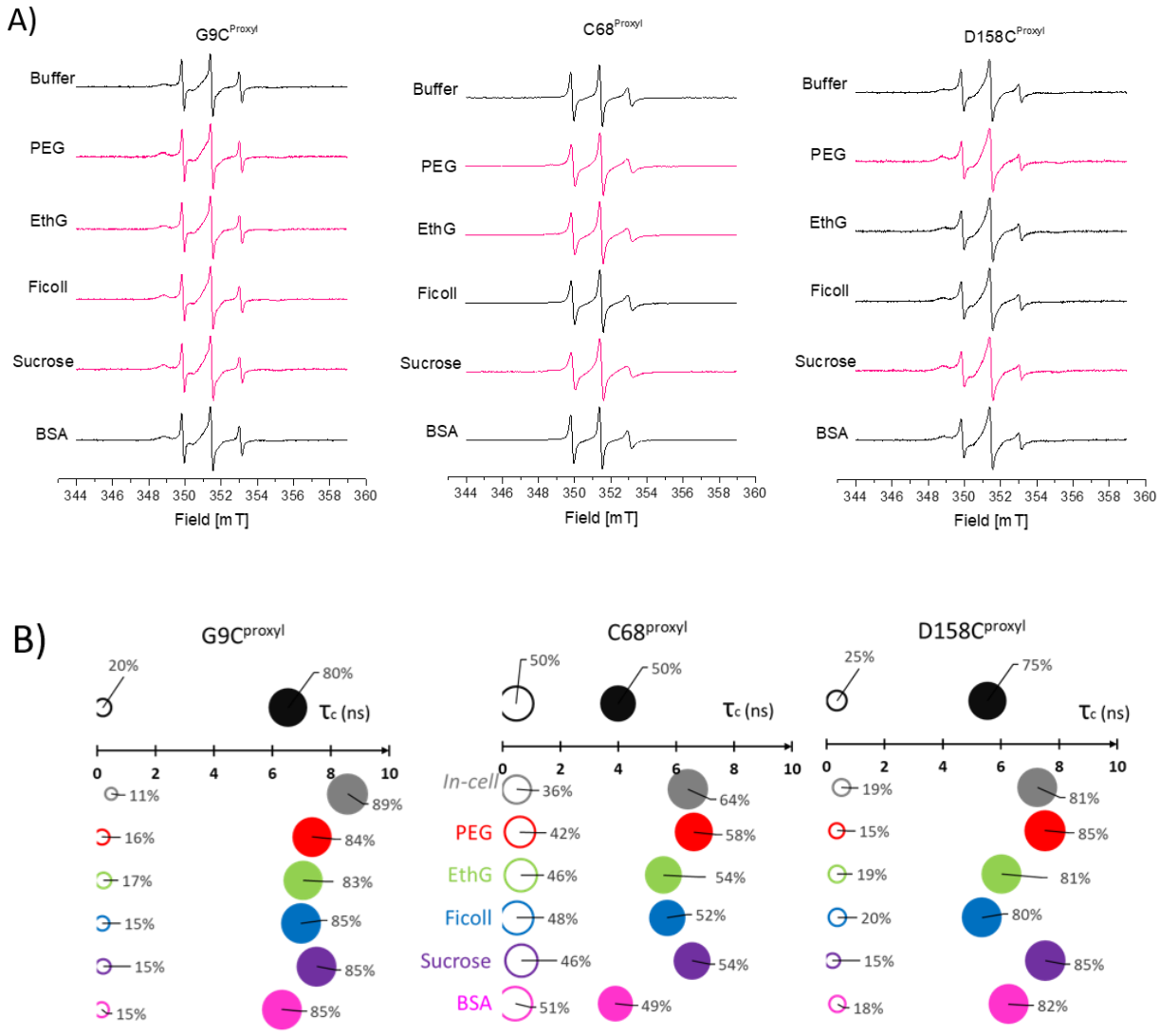

A) Room temperature, X-band CW-EPR spectra recorded for the studied UreG variants labeled with Proxyl in vitro (Tris Buffer 20mM, pH 7.4, NaCl 150 mM) and in the presence of crowding agents (PEG8000 200 mg/mL, Ethylene Glycole 20% v/v, Ficoll-70 300 mg/mL, Sucrose 30% w/v and BSA 300 mg/mL). If changes are detected upon crowder addition, spectra are indicated in magenta.
B) Results of the simulation of CW-EPR spectra (in panel A) of UreG variants. The sharper and broader components of the simulations are represented with an empty or full sphere, respectively. The EPR spectra of the variants in Tris are reported in black, *in-cell* in grey. The spectra in different conditions are colored as follows: in vitro (black), in-cell (grey) and in the presence of crowding agents: PEG8000 200 mg/mL (red); Ethylene Glycole 20% v/v (EthG, green), Ficoll 7000 200 mg/mL (blue); Sucrose 20% (purple); BSA 10 mg/mL (magenta). The population weight (%) is reported as area of the discs while the τ_c on the x-axis

Figure S9: in vitro DEER results for *Sp*UreG G9C^{proxyl}/D158C^{proxyl}, related to Figure 6.

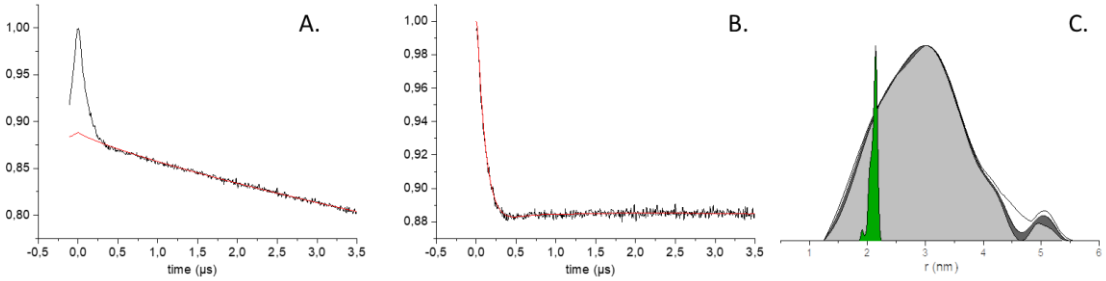

(A, B) Q-band DEER traces @ 60 K (*black*) and the baseline used for background correction (*red*). **(C)**The distance distributions were obtained using DeerAnalysis2019 and DEERNet (in *grey*),[1] while the distance distributions calculated by MMM software,[2] using the crystal structure available for *Helicobacter pylori* UreG and M-proxyl as spin label, are shown in *green.*

Figure S10: T_m measurements and Echo-Detected Field Sweeps (EDFS) related to Figure 6.

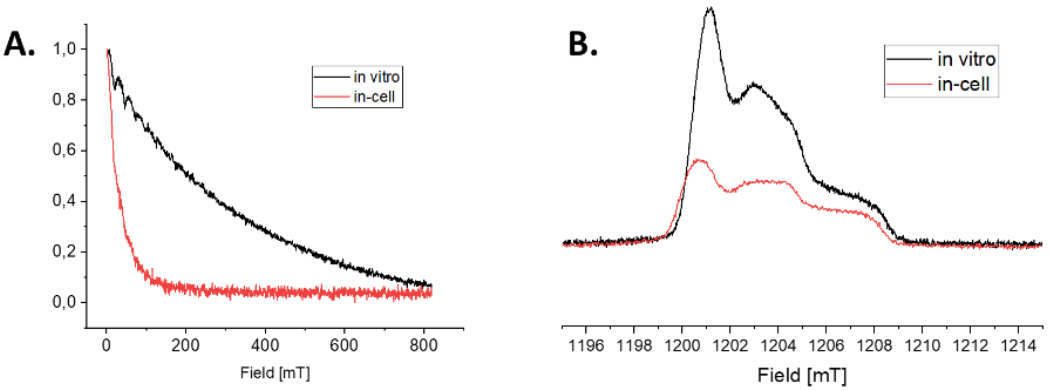

A) Q-band 2-pulses echo decay recorded at 60 K of *Sp*UreG-G9C^{proxyl}/D158C^{proxyl} labeled with M-Prox in dilute buffer solution (black line, Tris 20mM, pH 7.4, NaCl 150 mM, Glycerol 30 % v/v) and delivered by electroporation *in E. coli* cells (red line). Tm values are 3 µs and 0.3 µs for the samples in vitro and *in-cell*, respectively. **B)** Q-band Echo Field Sweep spectra recorded at 60 K of *Sp*UreG-G9C^{proxyl}/D158C^{proxyl} labeled with M-Prox in vitro (*black line*, Tris 20mM, pH 7.4, NaCl 150 mM, Glycerol 30 % v/v) and delivered by electroporation *red line in E. coli* cells.

Figure S11: DEER traces treatment, related to Figure 6.

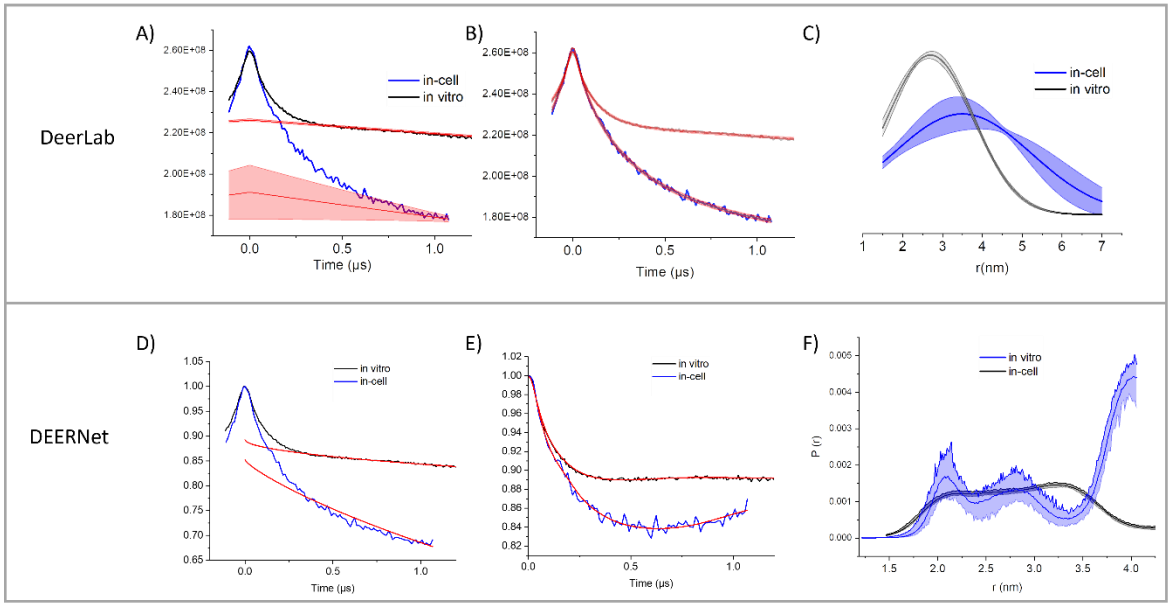

DEER data obtained for *Sp*UreG in vitro (black) and in *E. coli* cells (blue). DEER raw data were corrected using (A) DeerLab with a single Gaussian model[3] or (D) DEERNet.[1] The resulting fitting are shown in figures B) and E) respectively. The distances extracted are reported in panels C) and F) shaded gray and blue areas represent the uncertainty.

Simulation results of CW-EPR spectra, related to Figure 2.

All the spectra were simulated with SimLabel, a GUI of EasySpin. The EPR spectra presented in this work were simulated with the 'Slow Motion' mode of SimLabel. The EasySpin function used for spectra simulation was 'chili', while the used routine is described here: E. Etienne *et al. Magnetic Resonance in Chemistry* **2017**.[4]

Figure S12: Simulation results for C68^{prox} A) in vitro and B) *in-cell*.

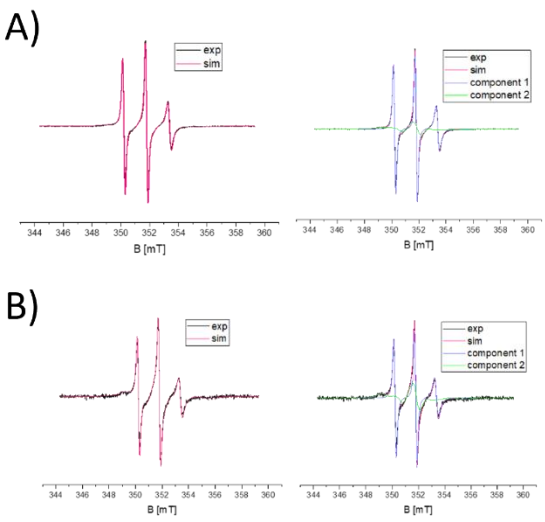

WT-C68 In Tris 10mM	component 1	component 2
tcorr	0,45 ns	4,0 ns
%	50%	50%
g	2,00886 2,00610 2,00220	2,00689 2,00610 2,00220
aN (mT)	0,42 0,42 3,94	0,48 0,48 4,00
aN_{iso} (mT)	1,59	1,65
Lw (mT)	G: 0,13 L:0,02	G:0,12 L:0,02

WT-C68 *in-cell*	component 1	component 2
tcorr	0,49 ns	6,4 ns
%	36%	64%
g	2,00922 2,00610 2,00220	2,00791 2,00610 2,00220
aN (mT)	0,40 0,40 3,97	0,55 0,55 3,75
aN_{iso} (mT)	1,59	1,62
Lw (mT)	G: 0,12 L:0,05	G:0,12 L:0,07

Figure S13: Simulation results for C68^{prox} in PEG8000.

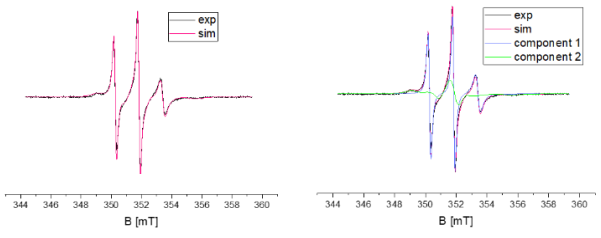

WT-C68 PEG8000	component 1	component 2
tcorr	0,6 ns	6,61 ns
%	41%	59%
g	2,00873 2,00610 2,00220	2,00746 2,00610 2,00220
aN (mT)	0,38 0,38 3,99	0,55 0,55 3,80
aN_{iso} (mT)	1,58	1,63
Lw (mT)	G: 0,07 L:0,05	G:0,12 L:0,12

Figure S14: Simulation results for C68^{prox} in Ethylene glycol.

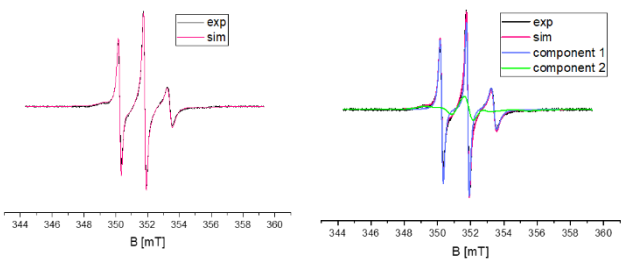

WT-C68 EthGly	component 1	component 2
tcorr	0,63 ns	5,56 ns
%	46%	54%
g	2,00884 2,00610 2,00220	2,00728 2,00610 2,00220
aN (mT)	0,39 0,39 3,97	0,55 0,55 3,76
aN_{iso} (mT)	1,59	1,62
Lw (mT)	G: 0,07 L:0,05	G:0,12 L:0,12

Figure S15: Simulation results for C68^{prox} in Ficoll 7000.

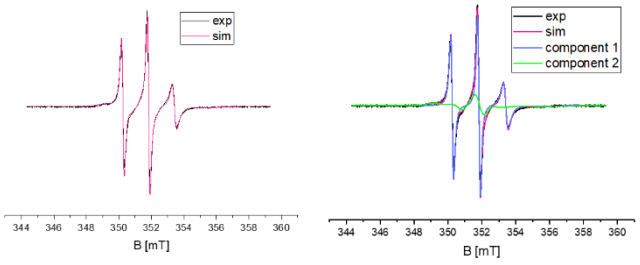

WT-C68 Ficoll7000	component 1	component 2
tcorr	0,50 ns	5,7 ns
%	48%	52%
g	2,00863 2,00610 2,00220	2,00747 2,00610 2,00220
aN (mT)	0,35 0,35 4,08	0,54 0,54 3,82
aN_{iso} (mT)	1,59	1,63
Lw (mT)	G: 0,07 L:0,05	G:0,12 L:0,07

Figure S16: Simulation results for C68^{prox} in Sucrose.

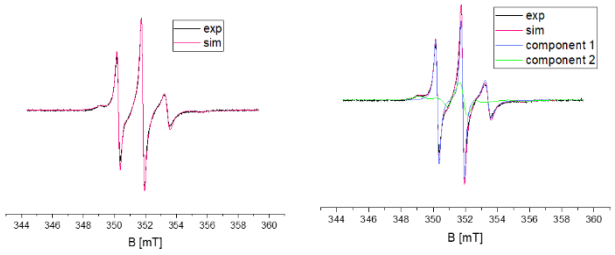

WT-C68 Sucrose20%	component 1	component 2
tcorr	0,65 ns	6,55 ns
%	46%	54%
g	2,00879 2,00610 2,00220	2,00751 2,00610 2,00220
aN (mT)	0,32 0,32 4,12	0,56 0,56 3,79
aN_{iso} (mT)	1,59	1,64
Lw (mT)	G: 0,08 L:0,06	G:0,02 L:0,01

Figure S17: Simulation results for C68^{prox} in Bovine Serum Albumin (BSA).

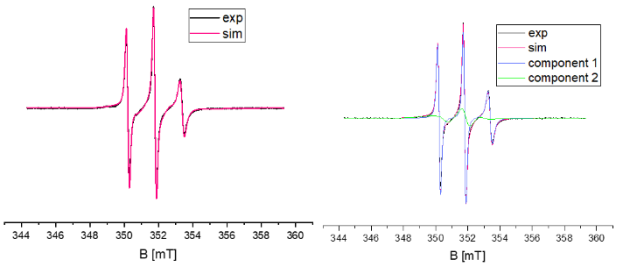

WT-C68 BSA	component 1	component 2
tcorr	0,42 ns	5,58 ns
%	44%	56%
g	2,00884 2,00610 2,00220	2,00707 2,00610 2,00220
aN (mT)	0,41 0,41 3,96	0,55 0,55 3,87
aN_{iso} (mT)	1,59	1,66
Lw (mT)	G: 0,12 L:0,05	G:0,07 L:0,07

Figure S18: Simulation results for G9C^{prox} A) in vitro and B) *in-cell*.

A)

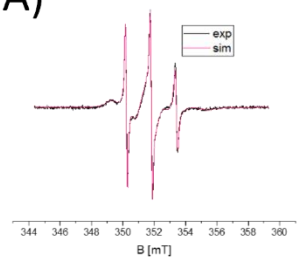

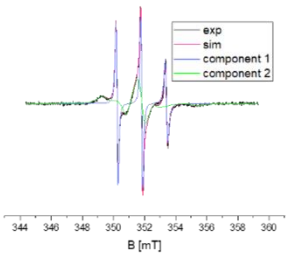

G9C In Tris 10mM	component 1	component 2
tcorr	0,20 ns	6,54 ns
%	21%	79%
g	2,00932 2,00610 2,00220	2,00874 2,00610 2,00220
aN (mT)	0,43 0,43 3,93	0,55 0,55 3,63
aN_{iso} (mT)	1,60	1,57
Lw (mT)	G: 0,08 L:0,09	G:0,01 L:0,01

B)

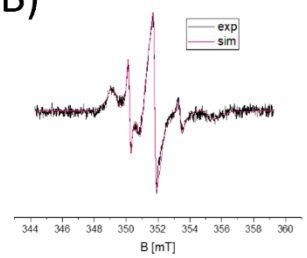

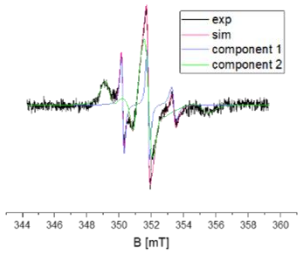

G9C *in-cell*	component 1	component 2
tcorr	0,41 ns	8,58 ns
%	11%	89%
g	2,00935 2,00610 2,00220	2,00890 2,00610 2,00220
aN (mT)	0,32 0,32 4,13	0,50 0,50 3,66
aN_{iso} (mT)	1,59	1,56
Lw (mT)	G: 0,08 L:0,09	G:0,01 L:0,01

Figure S19: Simulation results for G9C^{prox} in PEG8000.

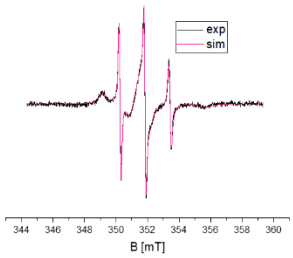

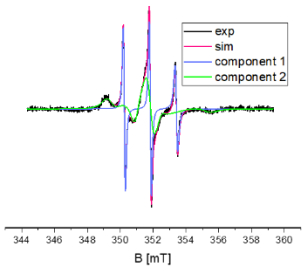

G9C PEG8000	component 1	component 2
tcorr	0,17 ns	7,36 ns
%	16%	84%
g	2,00941 2,00610 2,00220	2,00891 2,00610 2,00220
aN (mT)	0,34 0,34 4,04	0,53 0,53 3,68
aN_{iso} (mT)	1,59	1,58
Lw (mT)	G: 0,08 L:0,09	G:0,01 L:0,01

Figure S20: Simulation results for G9C^{prox} in Ethylene glycol.

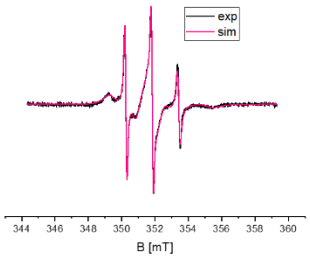

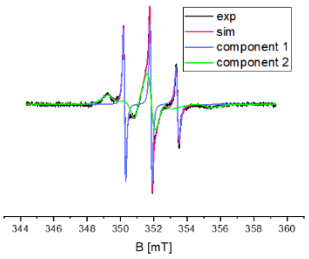

G9C EthGly	component 1	component 2
tcorr	0,21 ns	7,05 ns
%	17%	83%
g	2,00942 2,00610 2,00220	2,00868 2,00610 2,00220
aN (mT)	0,43 0,43 3,94	0,56 0,56 3,65
aN_{iso} (mT)	1,60	1,59
Lw (mT)	G: 0,01 L:0,01	G:0,01 L:0,01

Figure S21: Simulation results for G9C^{prox} in Ficoll 7000.

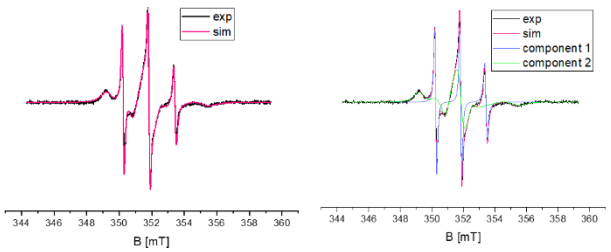

G9C Ficoll7000	component 1	component 2
tcorr	0,18 ns	6,98 ns
%	15%	85%
g	2,00932 2,00610 2,00220	2,00874 2,00610 2,00220
aN (mT)	0,43 0,43 3,93	0,55 0,55 3,69
aN_{iso} (mT)	1,60	1,60
Lw (mT)	G: 0,08 L:0,10	G:0,01 L:0,01

Figure S22: Simulation results for G9C^{prox} in Sucrose.

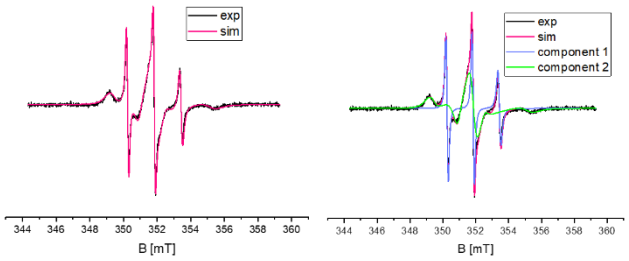

G9C Sucrose20%	component 1	component 2
tcorr	0,21 ns	7,52 ns
%	15%	85%
g	2,00932 2,00610 2,00220	2,00874 2,00610 2,00220
aN (mT)	0,43 0,43 3,93	0,55 0,55 3,67
aN_{iso} (mT)	1,60	1,59
Lw (mT)	G: 0,10 L:0,09	G:0,01 L:0,01

Figure S23: Simulation results for G9C^{prox} in Bovine Serum Albumin (BSA).

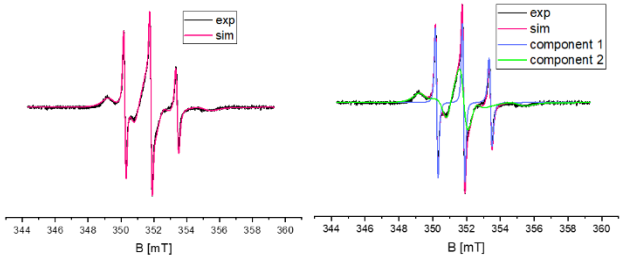

G9C BSA	component 1	component 2
tcorr	0,15 ns	6,33 ns
%	15%	85%
g	2,00940 2,00610 2,00220	2,00874 2,00610 2,00220
aN (mT)	0,35 0,35 4,10	0,56 0,56 3,73
aN_{iso} (mT)	1,60	1,62
Lw (mT)	G: 0,13 L:0,06	G:0,01 L:0,01

Figure S24: Simulation results for D158C^{prox} A) in vitro and B) *in-cell*.

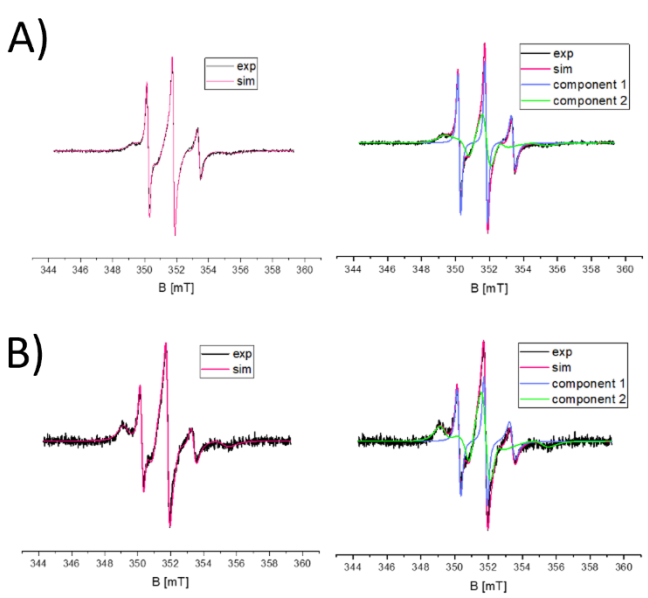

D158C Tris 10mM	component 1	component 2
tcorr	0,36 ns	5,53 ns
%	25%	75%
g	2,00938 2,00610 2,00220	2,00843 2,00610 2,00220
aN (mT)	0,32 0,32 4,14	0,55 0,55 3,66
aN_{iso} (mT)	1,60	1,59
Lw (mT)	G: 0,11 L:0,06	G:0,01 L:0,03

D158C *in-cell*	component 1	component 2
tcorr	0,52 ns	7,25 ns
%	19%	81%
g	2,00926 2,00610 2,00220	2,00870 2,00610 2,00220
aN (mT)	0,29 0,29 4,19	0,54 0,54 3,74
aN_{iso} (mT)	1,59	1,61
Lw (mT)	G: 0,13 L:0,06	G:0,01 L:0,03

Figure S25: Simulation results for D158C^{prox} PEG8000.

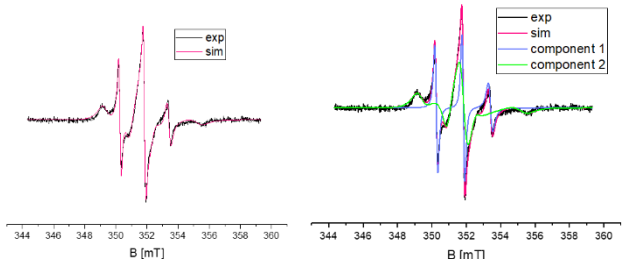

D158C PEG8000	component 1	component 2
tcorr	0,36 ns	7,51 ns
%	15%	85%
g	2,00945 2,00610 2,00220	2,00882 2,00610 2,00220
aN (mT)	0,30 0,30 4,15	0,55 0,55 3,73
aN_{iso} (mT)	1,58	1,61
Lw (mT)	G: 0,11 L:0,06	G:0,01 L:0,03

Figure S26: Simulation results for D158C^{prox} in Ethylene glycol.

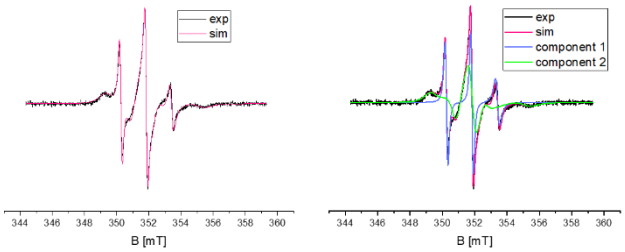

D158C EthGly	component 1	component 2
tcorr	0,37 ns	6,02 ns
%	19%	81%
g	2,00935 2,00610 2,00220	2,00842 2,00610 2,00220
aN (mT)	0,30 0,30 4,15	0,55 0,55 3,69
aN_{iso} (mT)	1,59	1,60
Lw (mT)	G: 0,11 L:0,06	G:0,01 L:0,03

Figure S27: Simulation results for D158C^{prox} in Ficoll7000.

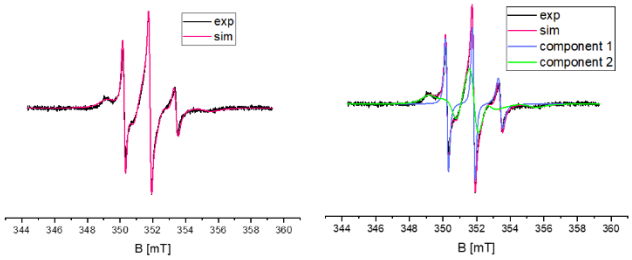

D158C Ficoll7000	component 1	component 2
tcorr	0,38 ns	5,34 ns
%	20%	80%
g	2,00938 2,00610 2,00220	2,00874 2,00610 2,00220
aN (mT)	0,32 0,32 4,14	0,55 0,55 3,86
aN_{iso} (mT)	1,60	1,65
Lw (mT)	G: 0,11 L:0,06	G:0,01 L:0,03

Figure S28: Simulation results for D158C^{prox} in Sucrose.

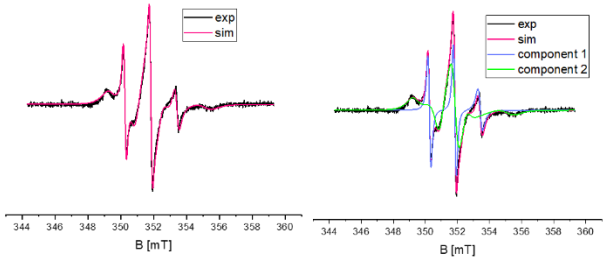

D158C Sucrose20%	component 1	component 2
tcorr	0,41 ns	6,10 ns
%	17%	83%
g	2,00934 2,00610 2,00220	2,00874 2,00610 2,00220
aN (mT)	0,29 0,29 4,19	0,55 0,55 3,75
aN_{iso} (mT)	1,59	1,62
Lw (mT)	G: 0,11 L:0,06	G:0,01 L:0,03

Figure S28: Simulation results for D158C^{prox} in Bovine Serum Albumin (BSA).

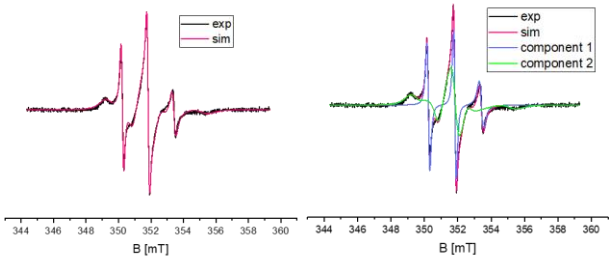

D158C BSA	component 1	component 2
tcorr	0,38 ns	6,26 ns
%	18%	82%
g	2,00938 2,00610 2,00220	2,00843 2,00610 2,00220
aN (mT)	0,32 0,32 4,14	0,55 0,55 3,74
aN_{iso} (mT)	1,60	1,61
Lw (mT)	G: 0,11 L:0,05	G:0,01 L:0,03

References

[1] S. G. Worswick, J. A. Spencer, G. Jeschke, I. Kuprov, *Science Advances* **2018**, *4*, eaat5218.

[2] G. Jeschke, *Protein Sci.* **2018**, *27*, 76-85.

[3] L. Fábregas Ibáñez, G. Jeschke, S. Stoll, *Magn. Reson.* **2020**, *1*, 209-224.

[4] E. Etienne, N. Le Breton, M. Martinho, E. Mileo, V. Belle, *Magnetic resonance in chemistry : MRC* **2017**, *55*, 714-719.